Surfactant Adsorption on Single-Crystal Silicon Surfaces in TMAH Solution: Orientation-Dependent Adsorption Detected by *In Situ* Infrared Spectroscopy

Prem Pal, Kazuo Sato, *Member, IEEE*, Miguel A. Gosalvez, Yasuo Kimura, Ken-Ichi Ishibashi, Michio Niwano, Hirotaka Hida, Bin Tang, and Shintaro Itoh

***Abstract*—This paper focuses on two aspects, *macroscopic and microscopic*, of pure and surfactant-added tetramethylammonium hydroxide (TMAH) wet etching. The macroscopic aspects deal with the technological/engineering applications of pure and surfactant-added TMAH for the fabrication of microelectromechanical systems (MEMS). The microscopic view is focused on the *in situ* observation of the silicon surface during etching in pure and surfactant-added TMAH solutions using Fourier transform infrared (FT-IR) spectroscopy in the multiple internal reflection geometry. The latter is primarily aimed at investigating the causes behind the change in the orientation-dependent etching behavior of TMAH solution when the surfactant is added. Silicon prisms having two different orientations ({110} and {100}) were prepared for comparison of the amount of adsorbed surfactant using FT-IR. Stronger and weaker adsorptions were observed on {110} and {100}, respectively. Moreover, ellipsometric spectroscopy (ES) measurements of surfactant adsorption depending on the crystallographic orientation are also performed in order to gain further information about the differences in the silicon–surfactant interface for Si{100} and Si{110}. In this paper, we determine the differences in surfactant adsorption characteristics for Si{110} and Si{100} using FT-IR and ES measurements for the first time, focusing both on the mechanism and on the technological/engineering applications in MEMS. [2009-0140]**

***Index Terms*—Anisotropic etching, ellipsometry, Fourier transform infrared (FT-IR) spectroscopy, IR, microelectromechanical systems (MEMS), silicon, surfactant, tetramethylammonium hydroxide (TMAH), Triton-X-100.**

I. Introduction

SILICON WET anisotropic etching has been an area of extensive research, particularly for the fabrication of microelectromechanical systems (MEMS)-based devices/systems. Numerous wet anisotropic etchants, such as potassium hydroxide water (KOH) [1], ethylenediamine pyrocatechol water (EDP or EPW) [2], hydrazine [3], ammonium hydroxide [4], cesium hydroxide water (CsOH) [5], and tetramethylammonium hydroxide (TMAH) [6], etc., have been studied. From an application point of view, three etching parameters are primarily considered to characterize the etchant, namely, the etch rate, the surface morphology, and the convex corner undercutting. The incorporation of surfactants, alcohols, and other additives to the etchant has been studied in order to alter the etching characteristics for specific applications, such as reducing the formation of hillocks or minimizing the undercutting at convex corners. Apart from the etching characteristics, toxicity, and cost of the etchant, a critical aspect is the clean room compatibility, particularly when the etching process is carried out after fabrication of complementary metal–oxide–semiconductor (CMOS) circuitry. Due to this, the TMAH solution has gained wide popularity, and recent research has concentrated on the effect of various kinds of surfactants, such as NC-200, Triton, PEG, ASPEG, etc. [7]–[12]. The addition of a very small amount of surfactant in TMAH, particularly at high concentration (i.e., 25 wt%), alters its etching characteristics considerably, in terms of undercutting at convex corners, curved edges, and straight edges aligned with non-$\langle 110 \rangle$ directions at Si{100} surface. It also reduces significantly the etch rate and improves the etched surface morphology of Si{110} surfaces, while not affecting noticeably those for Si{100}. Moreover, the surfactant addition significantly reduces the etch rate of vicinal Si{110} orientations, such as {221}, {331}, or {441}, while not strongly affecting vicinal Si{100} surfaces, such as {211}, {311}, or {411} [13]. This kind of etching characteristics provides a wide range of new shapes of MEMS structures [7], [8], [10], [14], [15]. However, the mechanism behind this change is still unclear, speculative—without experimental evidence—and a matter of debate [8], [10]. The experimental investigation of the etching mechanism, therefore, is essential to further accelerate the research in wet anisotropic etching and to promote its applications in silicon bulk micromachining for MEMS.

The change in the etching behavior of TMAH after the incorporation of the surfactant indicates that the reaction mechanism at the surface is affected by the surfactant molecules, which may block selectively some of the active surface sites, particularly those that appear on Si{110}. Fourier transform

Manuscript received May 28, 2009; revised July 30, 2009. First published October 20, 2009; current version published December 1, 2009. This work was supported in part by the Japan Society for the Promotion of Science through the Foreign Postdoctoral Research Fellowship Scheme (2008–2010) under Fellowship ID 08053 and in part by the Ministry of Education, Culture, Sports, Science and Technology (MEXT), Japan, under Grants-in-Aid for Scientific Research (A) 19201026 and 70008053. Subject Editor H. Seidel.

P. Pal, K. Sato, M. A. Gosalvez, H. Hida, B. Tang, and S. Itoh are with the Department of Micro/Nano Systems Engineering, Nagoya University, Nagoya 464-8603, Japan (e-mail: prem@mech.nagoya-u.ac.jp; sato@mech.nagoya-u.ac.jp; mag@coe.mech.nagoya-u.ac.jp).

Y. Kimura and M. Niwano are with the Research Institute of Electrical Communication, Tohoku University, Sendai 980-8577, Japan (e-mail: ykimura@riec.tohoku.ac.jp; niwano@riec.tohoku.ac.jp).

K.-I. Ishibashi was with the Research Institute of Electrical Communication, Tohoku University, Sendai 980-8577, Japan. He is currently with Hang-ichi Co. Ltd, Yokohama, Japan (e-mail: ikenichi@riec.tohoku.ac.jp).

Color versions of one or more of the figures in this paper are available online at http://ieeexplore.ieee.org.

Digital Object Identifier 10.1109/JMEMS.2009.2031688

infrared (FT-IR) spectroscopy is an effective tool to investigate the bonding and adsorption of foreign molecules at the surface under observation [16]–[27]. Attenuated total reflection IR spectroscopy is a very promising method for the *in situ* analysis of the surface. It has been demonstrated for real-time observation of silicon etching/cleaning/oxidation processes [16]–[26]. In addition, we consider ellipsometric spectroscopy (ES) measurements since this technique is able to characterize the thickness of thin adsorbed layers on surfaces at the subnanometer scale [28].

This paper focuses on two aspects, macroscopic and microscopic, of surfactant-added TMAH. On the one hand, the relevance for MEMS applications by fabricating new shapes of structures—which are not possible by conventional wet etching using pure TMAH (or KOH) solutions—is considered. This is termed as the "macroscopic aspects." On the other hand, a microscopic perspective in this paper is the *in situ* observation of the Si/TMAH and Si/(TMAH+surfactant) interfaces during etching using FT-IR spectroscopy in the multiple internal reflection (MIR) geometry to detect the selective adsorption of surfactant on different crystallographic planes. In addition to the FT-IR study, ellipsometric measurements are also performed on different orientations treated in surfactant-added water solution. The combined FT-IR and ellipsometric study is referred to as the "microscopic aspects." This paper is part of a major effort to find out the mechanism behind the following: 1) the etch rate reduction for vicinal and exact Si{110} surfaces and 2) the relative stability of the etch rate for vicinal and exact Si{100} orientations, when the surfactant is added in high-concentrated TMAH. In this paper, we focus on the experimental verification of the preferential adsorption of the surfactant on the different surface orientations. Triton-X-100 is selected as the surfactant due to its nonionicity in order to maintain the post CMOS process compatibility of TMAH solution. In addition, Triton remains in liquid phase at room temperature, making it easy to measure volumetrically and to mix in the solution. Triton-X-100 (iso-octylphenoxy polyethoxyethanol) has the following molecular structure:

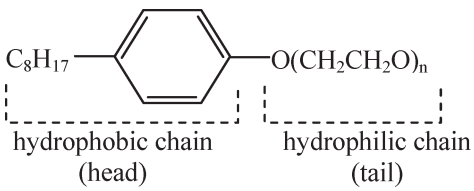

One end of the molecule is hydrophilic, and the other is hydrophobic.

II. Experimental Procedure

P-type Czochralski-grown silicon wafers with {100} and {110} orientations are used for both the macroscopic (application-oriented) and microscopic (surfactant adsorption selectivity) studies. A 25-wt% TMAH and a Triton-X-100 $[C_{14}H_{22}O(C_2H_4O)_n, n = 9 - 10]$ are selected as the main etchant and surfactant, respectively. We refer to the 25-wt% TMAH aqueous solution as *pure TMAH* and to the aqueous solution of 25-wt% TMAH with 0.1% v/v of Triton as *surfactant-added TMAH*. A constant temperature water bath is used to monitor the etchant temperature $(\pm 1\ ^\circ\mathrm{C})$. A Teflon container equipped with a reflux condenser is used for both etching solutions. In order to demonstrate the technological applications of pure and surfactant-added TMAH for the realization of various MEMS components, oxidized silicon wafers are patterned photolithographically and etched in buffered hydrofluoric (BHF) acid for oxide removal. The patterned chips are cleaned chemically and rinsed thoroughly in deionized (DI) water. Immediately before immersing in the etchant, they are dipped in 5% HF to remove any trace amount of native oxide. The total etching time for a desired etch depth depends on the etch rate for the specific temperature.

To investigate the effect of Triton, particularly on the etch rates of {100} and {110} crystallographic planes, IR spectroscopic measurements were carried out at room temperature in the attenuated total reflectance configuration [16]–[27]. Fig. 1 shows a schematic view of the process steps used for the preparation of silicon samples of different orientations (i.e., silicon prisms) of $40 \times 10 \times 0.5$ mm^3 in size with 45° bevels cut at the short edges. First, a thick silicon oxide layer of about 3 μm was grown by thermal oxidation process and patterned by photolithography followed by oxide etching in BHF acid. As shown in the experimental arrangement of the measurement system (Fig. 2), an O-ring made of Nitrile rubber is used to seal the Teflon cell in order to make it liquid leakage free. The use of a thick oxide [as shown in Figs. 1(b) and 2(b)] avoids the detection of absorption peaks from the O-ring. After oxide patterning, the positive photoresist is spin coated to avoid any scratch during further processing steps. The photoresist coated wafers are then diced to make the rectangular pieces of 40×10 mm^2 size. After this step, both ends are beveled by mechanical and chemical polishing processes. The samples are then cleaned properly.

In order to collect the background spectra of TMAH (or TMAH+Triton) and DI water, a very thin layer (1–2 nm) of oxide is grown by dry thermal oxidation to prevent direct contact with the silicon surface which would be otherwise etched. The sample is mounted into a Teflon cell and fitted into the experimental system, as shown in Fig. 2. The silicon prism, as shown in Fig. 2(b), provides MIRs during the measurements. The Teflon cell used in this experiment is custom made. The IR spectra are then collected for different states of the silicon surface. When the spectra are collected, the solution is continuously supplied through a pipe and drained to another pipe connected to the outlet. The measurement scheme is summarized as follows.

1) IR spectrum while sample (with thin oxide) is exposed to dry air only.
2) IR spectrum while flowing DI water.
3) IR spectrum while flowing TMAH (or TMAH+Triton), followed by the following:
   a) cleaning of the sample surface by successive flow of DI water;
   b) removal of thin oxide (1–2 nm) by flowing 5% HF followed by thorough rinse using flowed DI water.
4) IR spectrum while flowing DI water.

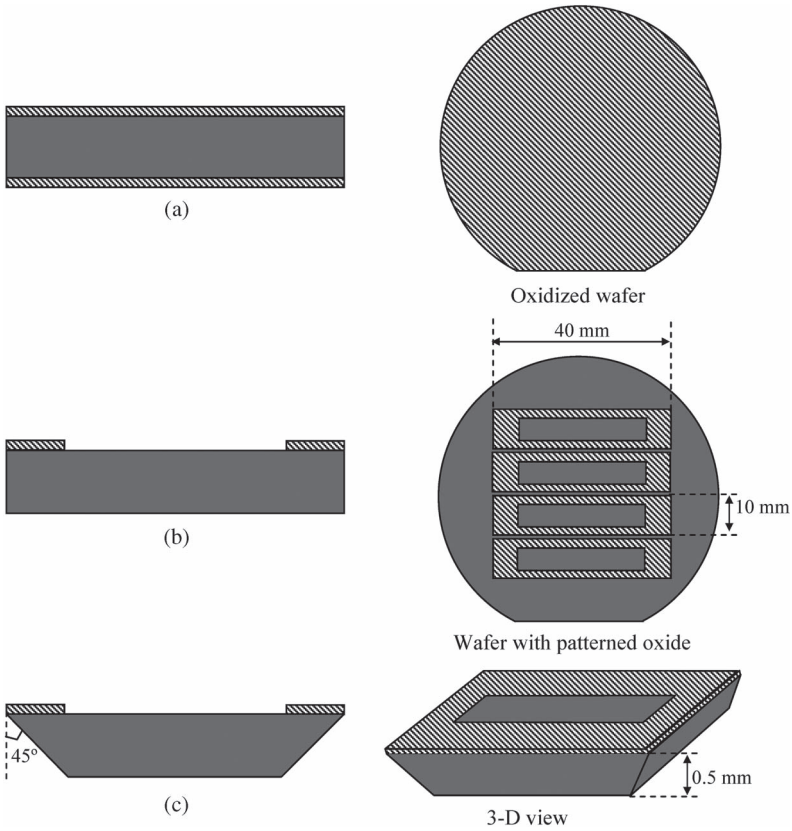

Fig. 1. Process steps for the fabrication of oxide-patterned silicon prisms. (a) Thermal oxidation in order to deposit 3-μm-thick oxide layer. (b) Photolithography for oxide patterning and dicing of wafer. (c) 45° beveling of both ends by mechanical and chemical polishing.

5) IR spectra while flowing TMAH or (TMAH+Triton). At this step, 8–10 spectra are collected after every 2 min in order to observe the effect of etching with time, followed by the following:
   a) thorough rinsing by flowing DI water.
6) IR spectrum while flowing DI water, followed by the following:
   a) 5% HF treatment;
   b) thorough rinsing by flowing DI water.
7) IR spectrum while flowing DI water.

In order to gain further information about the differences in the silicon–surfactant interaction for Si{100} and Si{110}, *ex situ* ES measurements are performed. For this purpose, 1%-v/v Triton is added into DI water. In this case, Triton is not added to the TMAH solution in order to isolate the silicon–surfactant system and to characterize the thickness of the surfactant layer formed over the silicon surface. The silicon samples are cleaned properly and dipped in 5% HF to remove any trace amount of oxide followed by a thorough rinse in DI water. The samples are then dipped in the surfactant-added DI water for 15 min. This time was optimized by measuring the surfactant layer thickness for different dipping times. It was observed that the thickness becomes saturated after 7–8 min. Thereafter, samples are taken out and rinsed by dipping in pure DI water several times (three to four). We refer to the overall treatment consisting in cleaning + dipping in Triton-added DI water + rinsing as the "surfactant treatment." Finally, the samples are dried in air and placed in the spectroscopic ellipsometry analyzer (MARY-102). ES measurements for clean Si{100} and Si{110} surfaces—prepared by dipping in 5% HF followed by a thorough rinse in DI water to rule out any possibility of native oxide layer—are used as reference for Si{100}/Triton and Si{110}/Triton, respectively.

III. Results

A. Macroscopic Aspects (Application-Oriented Studies)

First, the etching characteristics in pure 25-wt% and 0.1%-v/v Triton-added TMAH, as shown in Figs. 3–5, are measured to emphasize the motivation of this paper. As shown in Fig. 3, the etch rate of Si{100} remains almost unchanged in both cases, while the Si{110} etch rate decreases to a significantly low level in Triton-added TMAH. The addition of Triton reduces the undercutting at sharp convex and rounded concave corners markedly (Fig. 4). The etched surface morphologies of {100} and {110} in pure and Triton-added TMAH are shown in Fig. 5. For {100}, no noticeable change is observed when the Triton is added, whereas {110} becomes smoother. The undercutting at sharp convex corners occurs due to the emergence of high index planes. The amount of undercutting is different in pure and surfactant-added TMAH, being significantly low for surfactant-added TMAH. An explanation for this behavior is presented in Section IV.

In order to illustrate the technological/engineering applications of both types of etchants, different shapes of masking patterns are etched in {100}-oriented silicon wafers. If the etch rate of {110} is very low in comparison to {100}, as in Fig. 3

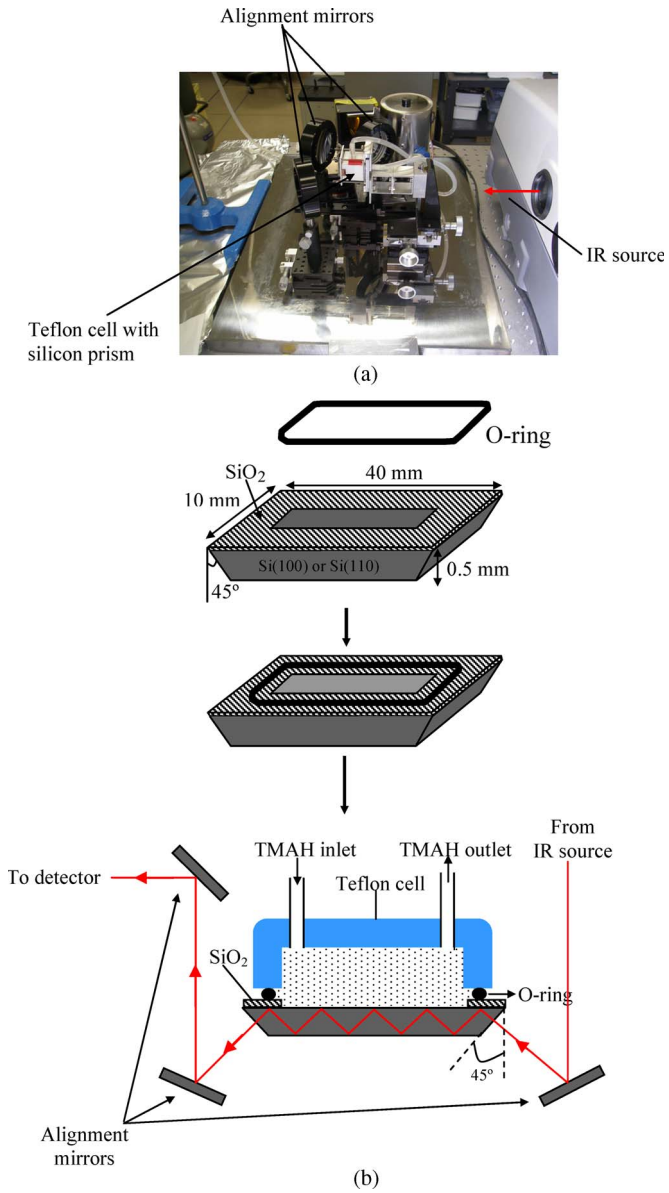

Fig. 2. FT-IR experiment setup for *in situ* measurements of silicon etching behavior in pure and Triton-added TMAH. (a) Optical photograph. (b) Schematic.

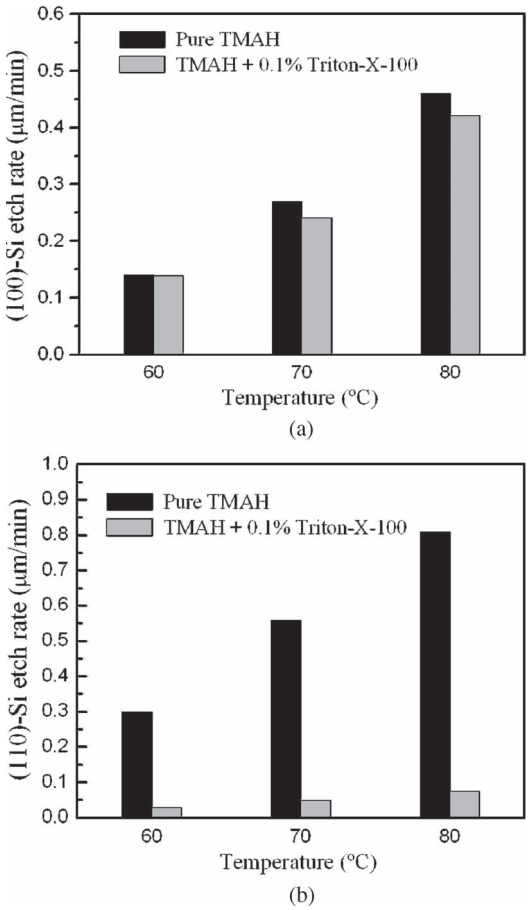

Fig. 3. Comparison of the etch rates of (a) Si{100} and (b) Si{110} at different temperatures. When Triton is added in TMAH, the etch rate of Si{100} is almost unaffected, while that for Si{110} is suppressed significantly.

for TMAH+Triton, {110} emerges at the mask edges aligned with the ⟨100⟩ direction, making an angle of 45° with the {100} wafer surface. This is suitable for the fabrication of 45° mirrors, as shown in Fig. 6. The significantly low undercutting at the convex and rounded concave corners in TMAH+Triton can be beneficially used to etch conformally any arbitrarily shaped pattern down to a depth of 20–25 μm. As an example, SEM photographs of fabricated serpentine microfluidic channels and microstructures with sharp convex and rounded concave corners are shown in Fig. 7. An interesting feature of surfactant-added TMAH is also demonstrated by micromachining alphabet letters, as shown in Fig. 8. The shapes of the letters are correctly maintained down to a certain etch depth (depending on the actual size of the letters), after which slanted sidewalls merge with each other. In order to make suspended structures using P^+-Si (or SiO_2/Si_3N_4), high undercutting is desirable for their fast release. In that case, pure TMAH is an appropriate choice as it provides very high undercutting. Hence, pure and surfactant-added TMAH provide two good choices for the formation of different shapes of MEMS structures, depending on the actual requirements.

B. Microscopic Phenomena (Surfactant Adsorption Selectivity)

The novelty of this paper resides in the *in situ* observation of the silicon surface during etching using FT-IR spectroscopy. In order to observe the status of {100} and {110} under different conditions during the experiments, the following absorbance spectra were calculated from the measurement scheme presented in Section II:

1) IV-II in order to observe the surface before etching;
2) V-III for investigating the surface during etching;
3) VII-II for the observation of hydride states after etching.

Here, "IV-II" means that the spectra collected at step II are subtracted from those collected at step IV. Fig. 9 shows the IR spectra of Si{100} and Si{110} in the Si-H_2 and Si-H absorption regions before etching (IV-II). The absorbance spectra of {100} and {110} taken after every 2 min during etching in pure and Triton-added TMAH (V-III) are shown in Fig. 10. After etching in pure and surfactant-added TMAH, the IR spectra in

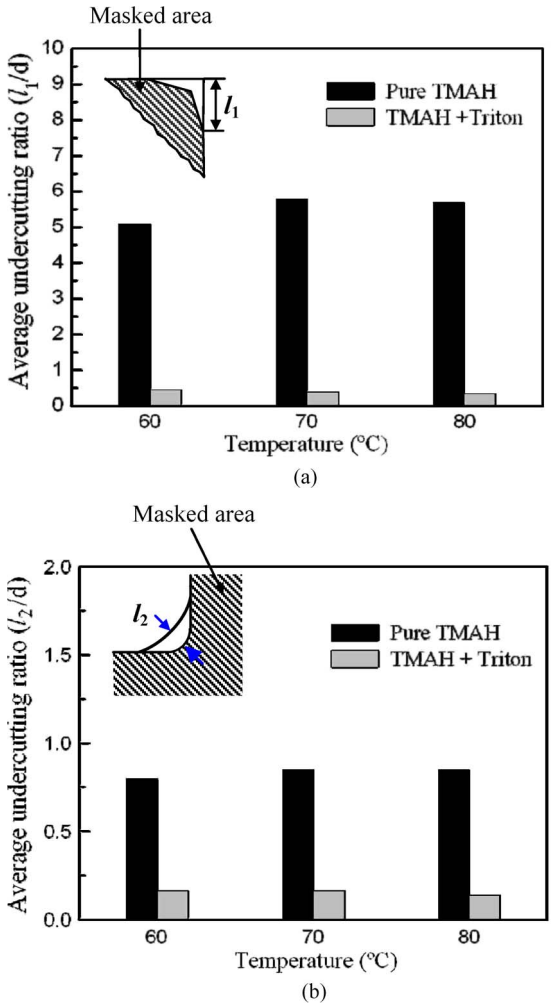

Fig. 4. Comparison of the undercutting ratio in pure and Triton-added TMAH solutions for (a) l_1/d at convex corners and (b) l_2/d at rounded concave corners on Si{100} at different temperatures. l_1 is the undercutting along $\langle 110 \rangle$ direction at convex corner. l_2 is the undercutting along $\langle 100 \rangle$ direction at rounded concave corner. d is the etch depth.

the Si-H_2 and Si-H regions after washing (performed by flowing 5% HF followed by DI water) are shown in Fig. 11 (VII-II). In this figure, the absorbance spectrum for Si{110} etched in pure TMAH could not be measured correctly due to the rough morphology. In addition, Fig. 12 shows a comparison of the surfactant layer thickness on the {110} and {100} surfaces after the surfactant treatment at different temperatures. The thickness is measured *ex situ* by ES.

IV. Discussion

In this section, we show that the strong reduction in the etch rate and surface roughness of Si{110} and the weak effects for Si{100} are also valid for their corresponding vicinal surfaces. This is done by performing the following: 1) providing references to earlier published etch rates and surface morphologies for the vicinal orientations; 2) presenting the major resembling features between the crystallographic structures within each vicinal family; and 3) analyzing the change in the etched profile with and without the surfactant in our experiments. The cross-analysis suggests that the exact and vicinal Si{110} surfaces are protected by an adsorbed surfactant layer, while the exact and vicinal Si{100} orientations are weakly affected. This conclusion is confirmed by analyzing the FT-IR and ES results. Finally, a simple model is proposed in order to explain the change in the etching characteristics when the surfactant is added in TMAH.

As mentioned in Section III-A, the etch rate of Si{110} is strongly reduced when Triton is incorporated in TMAH, while the Si{100} etch rate is almost unaffected (Fig. 3). The results for Si{110} can directly be correlated to other orientations, such as {441}, {331}, or {221}, as their etch rates are also reduced significantly in other etchants containing TMAH and other surfactants [13], [29]. These orientations are examples of the $\{h\ h\ 1\}$ and $\{h+2\ \ h+2\ \ h\}$ surface families with $h \geq 3$ and $h \geq 2$, respectively, appearing between {110} and {111} and characterized by having reduced etch rates and smooth etched surface morphologies in TMAH+surfactant in general. From a crystallographic point of view, all these surfaces are characterized by containing Step Monohydride (SM) and Terrace Monohydride (TM) sites in varying amounts, with {110} and $\{h\ h\ 1\}$ being SM rich while $\{h+2\ \ h+2\ \ h\}$ and {111} are TM rich [29]–[31]. Due to the similar effect caused by the addition of the surfactants and the crystallographic similarities between these surfaces, we choose to refer to them in this paper as vicinal {110} orientations. Similarly, other orientations such as {411}, {311}, and {211} are examples of the $\{h\ \ 1\ \ 1\}$ and $\{h+2\ \ \ h\ \ \ h\}$ surface families with $h \geq 3$ and $h \geq 2$, respectively, appearing between {100} and {111} and characterized by having etch rates and surface morphologies that are not significantly affected by the addition of the surfactants in general, as shown in Fig. 3(a) for the particular case of {100} [13], [29].

Fig. 13 shows the difference in the undercutting planes formed at $\langle 100 \rangle$-oriented mask edges in pure TMAH and surfactant-added TMAH. The sidewalls are 90°-inclined {100} planes in Fig. 13(a) for pure TMAH while they are 45°-inclined {110} planes in Fig. 13(b) for TMAH+Triton. The angle of inclination of the sidewalls correlates with the location of the minimum etch rate for all planes that contain the $\langle 100 \rangle$ direction of the mask edge, i.e., the minimum of the etch rate in the $\langle 100 \rangle$ crystallographic zone. This minimum is located at {100} for pure TMAH while it is located at {110} for surfactant-added TMAH. In a similar manner, Fig. 7(b)(i) shows that, for pure TMAH, the undercutting at the convex corners is controlled by the {311} fast etching plane (i.e., a vicinal {100} plane), while Fig. 7(b)(ii) shows that the undercutting is controlled by vicinal {110} planes, namely, {221}, {331}, {441}, etc. Since the etch rates of these planes are 1) very low and 2) very similar, the amount of undercutting is dramatically reduced, and only a round profile can be observed (none of the planes can stand out clearly from the rest). This shows that the exact and vicinal {110} planes have low etch rates, in agreement with other experiments [13], [29], indicating that this family of surfaces is protected by the surfactant molecules during etching. As discussed in the following, this is due to the formation of a surfactant layer that is more strongly adsorbed on the {110}, $\{h\ h\ 1\}$, and $\{h+2\ \ h+2\ \ h\}$ surfaces than on the {100}, $\{h\ 1\ 1\}$, and $\{h+2\ \ h\ \ h\}$ surfaces.

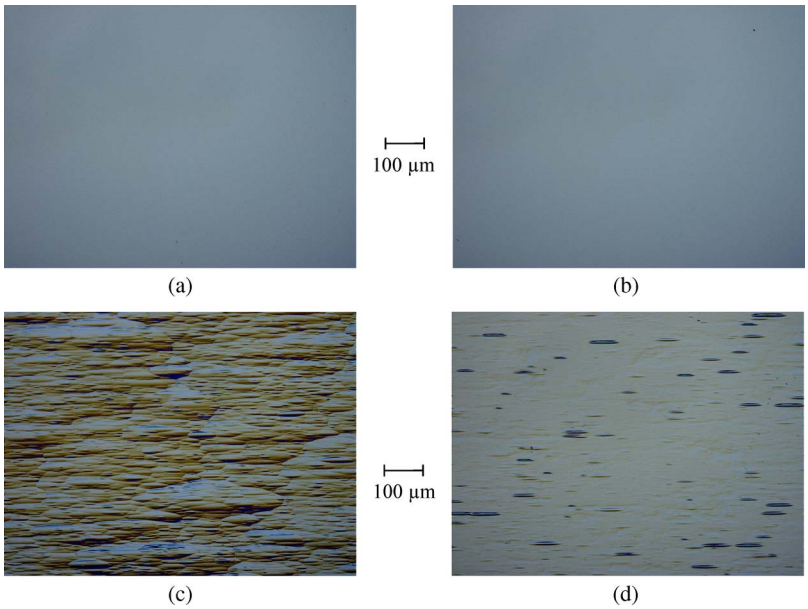

Fig. 5. Optical photographs of etched surface morphologies in pure and surfactant-added TMAH. (a) {100}-Si in pure 25% TMAH ($Ra = 8$ nm). (b) {100}-Si in 25% TMAH+Triton-X-100 ($Ra = 9$ nm). (c) {110}-Si in pure 25% TMAH ($Ra = 530$ nm). (d) {110}-Si in 25% TMAH+Triton-X-100 ($Ra = 73$ nm).

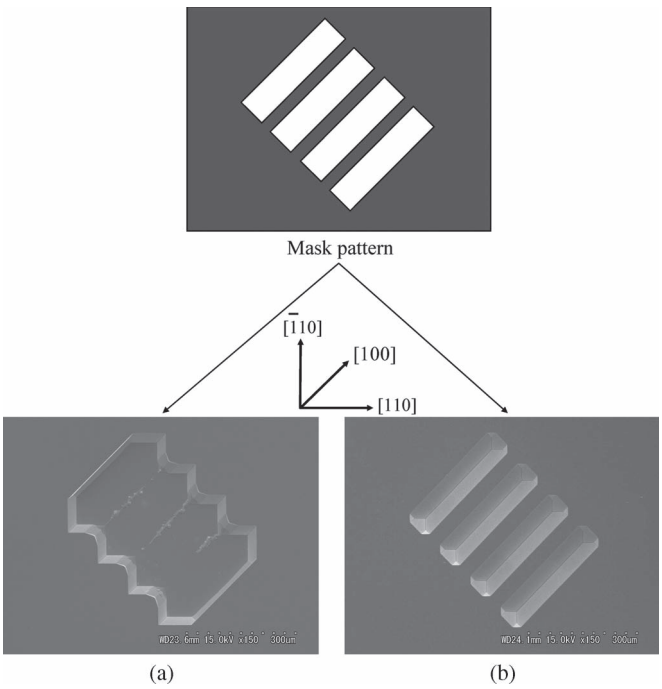

Fig. 6. Fabrication of 45° mirror in (a) pure and (b) Triton-added TMAH. The etched profile in (b) demonstrates that the etch rate of Si{110} is much smaller than that of Si{100}, as also shown in Fig. 3.

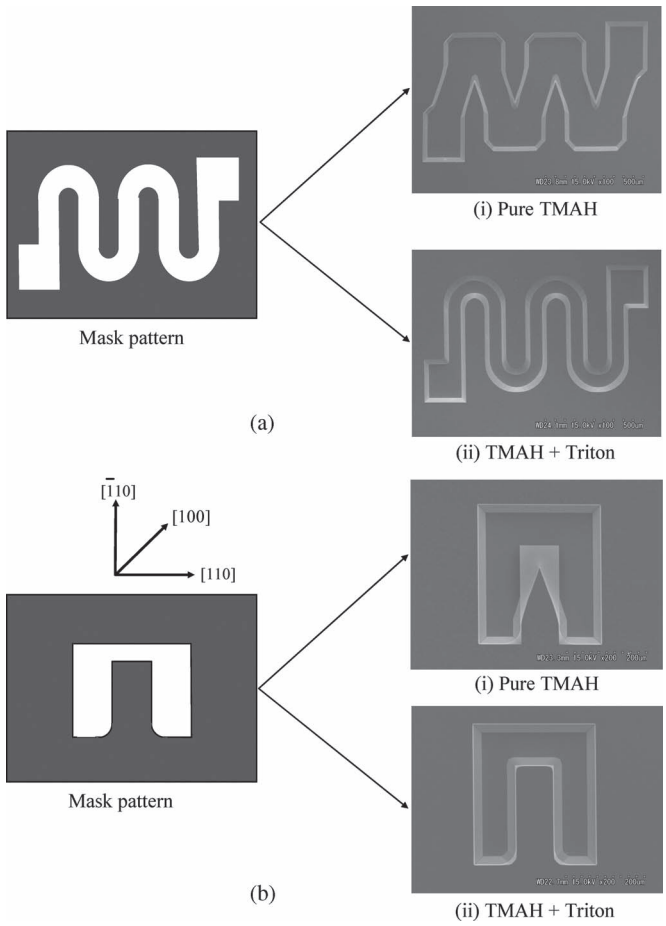

Fig. 7. Fabrication of (a) serpentine-shaped microfluidic channels and (b) cantilever beams with sharp convex and rounded concave corners on Si{100} in pure and Triton-added TMAH. This demonstrates the direct application of low and high undercutting, as shown in Fig. 4, for MEMS applications.

The previous macroscopic aspects need microscopic confirmation in order to verify the preferential adsorption of the surfactant molecules on {110}, as compared to {100}. As mentioned earlier FT-IR spectroscopy is one of the powerful methods that can be used to investigate the surface under investigation. As shown in Fig. 9, before etching, the absorption peaks for dihydride and monohydride termination for Si{100} and Si{110} appear dominantly at 2110 and 2070 cm^{-1}, respectively. During etching, these peaks appear at 2077 and 2045 cm^{-1}, respectively, due to the change in the local environment from DI water only to aqueous TMAH, which contains TMA^+ and OH^- ions in addition to water. Moreover, the peak heights for Si-H and Si-H_2 are reduced during the etching in comparison to those before etching. As reported,

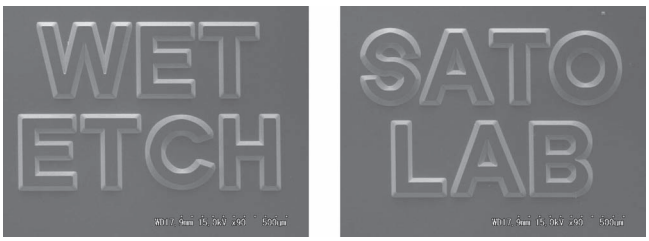

Fig. 8. Micromachining of alphabet letters in surfactant-added TMAH (etch depth $= 30\ \mu$m).

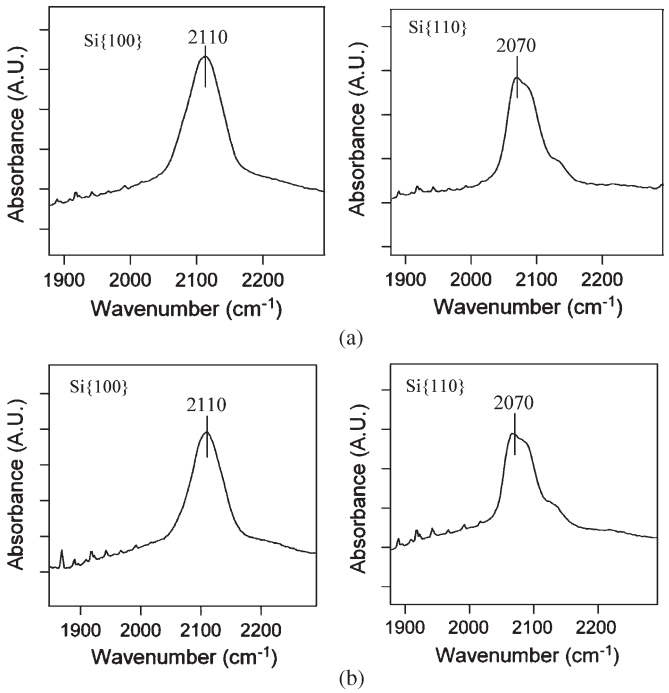

Fig. 9. IR absorption spectra in Si-H and Si-H_2 vibration regions for Si{100} and Si{110} before etching in (a) TMAH and (b) TMAH+Triton. In both cases, the surfaces are exposed to DI water after 5% HF treatment. (a) Before etching in pure TMAH. (b) Before etching in TMAH+Triton.

hydrogen-terminated surfaces are very susceptible to the local environment, and various parameters for different solvents (such as the dielectric constant, Gutmann's electron-donor and electron-acceptor numbers, etc.) are considered to be responsible for the IR frequency shifts [27], [32]. Generally, the dielectric effects are widely accepted as an explanation. As an example, Ozanam *et al.* studied the frequency shift in the presence of various solvents, showing good agreement with our results [27]. The shifted peaks at 2077 and 2045 cm^{-1} are attributed to strained dihydride and monohydride states of silicon surfaces, respectively [27], [33]. The spectra above 3000 cm^{-1} show only broad depressions around 3300 cm^{-1} due to absorbance by water.

In the case of etching in TMAH+Triton, the same shifts in the IR frequency for the dihydride $(Si\text{-}H_2)$ and monohydride (Si-H) states are detected. However, additional peaks corresponding to C-H vibrational modes are also observed, as shown in Fig. 10(c) and (d). The peaks at 2874 and 2950 cm^{-1} are attributed to the CH_3 symmetric and asymmetric stretch modes, respectively [34]. These additional peaks unambiguously reveal the presence of Triton on the surface [16], [17], [26]. By comparing their intensities for Si{100} and Si{110}, we conclude that Triton is adsorbed more strongly on Si{110}. As a result, the {110} planes are significantly prevented from being attacked by H_2O and OH^- during etching, resulting in a reduced etch rate, as shown in Fig. 3(b). Since Triton does not adsorb as strongly on Si{100}, the corresponding reduction of the etch rate is much weaker, as shown in Fig. 3(a).

The *in situ* observation of the silicon surface during etching in this paper confirms the existence of the selective adsorption of the surfactant molecules. The difference in the surfactant layer thickness for Si{110} and Si{100} measured by spectroscopic ellipsometry after the surfactant treatment, as shown in Fig. 12, validates the orientation-dependent adsorption of the surfactant molecules. The figure shows that the surfactant layer formed on Si{110} is thicker than on Si{100}, indicating once more a stronger attachment to the surface. After etching (Fig. 11), the surfaces treated in 5% HF and rinsed in DI water display dihydride and monohydride absorption peaks at the corresponding wavenumbers as previously observed (Fig. 9), indicating that the surfaces are returned to the expected H-termination states.

It is known that the surface of silicon is mostly H-terminated during etching [35], [36] and that H-terminated surfaces are characteristically hydrophobic [18]. It is also well known that the surfactant molecules will adsorb on a hydrophobic surface by forming an adsorbed layer, where the hydrophobic part of the molecules (or head) is in contact with the surface while the hydrophilic part (or tail) remains in contact with water [16], [37]. Traditionally, the layer thickness from ellipsometry studies is known to reflect the density of adsorbed molecules (adsorption density), related to the larger (more perpendicular) or smaller (more oblique) degree of packing of the molecules. On the other hand, the wavenumber of an FT-IR absorbance peak reflects the kind of bond and its vibrational mode, whereas the relative intensity of the peak can reflect either stronger physisorption (bringing the species closer to the surface) or a larger density, or both (in addition to the relative alignment between the radiation and the bonds). Our combined study strongly indicates that the surfactant molecules preferentially adsorb on Si{110}, exhibiting a larger packing density and stronger physisorption.

At the molecular level, a further explanation of the preferential adsorption of the surfactant is as follows. For fully H-terminated surfaces, we argue that the only forces between the water molecules and an H-terminated silicon surface are weak hydrogen bonds between surfacial $Si^{\varepsilon+}$ and aqueous $O^{\delta 2-}$ and between surfacial $H^{\varepsilon-}$ and aqueous $H^{\delta+}$. Here, δ (delta) and ε (epsilon) refer to *small* and *very small* charges, respectively, due to the differences in electronegativities between O and H in water and between Si and H at the surface, respectively. Although these interactions are weak, they are localized at H-terminations. We calculate the number of H-terminations per unit area for the crystallographic cut of Si{100} and Si{110} as $4/a^2$ and $4/(a^2\sqrt{2})$, respectively, where a is the lattice parameter of the conventional unit cell. This simple calculation suggests that Si{110} is more hydrophobic (lower H-density) than Si{100}. If the water and surfactant molecules are to compete for suitable locations over the surface, on average,

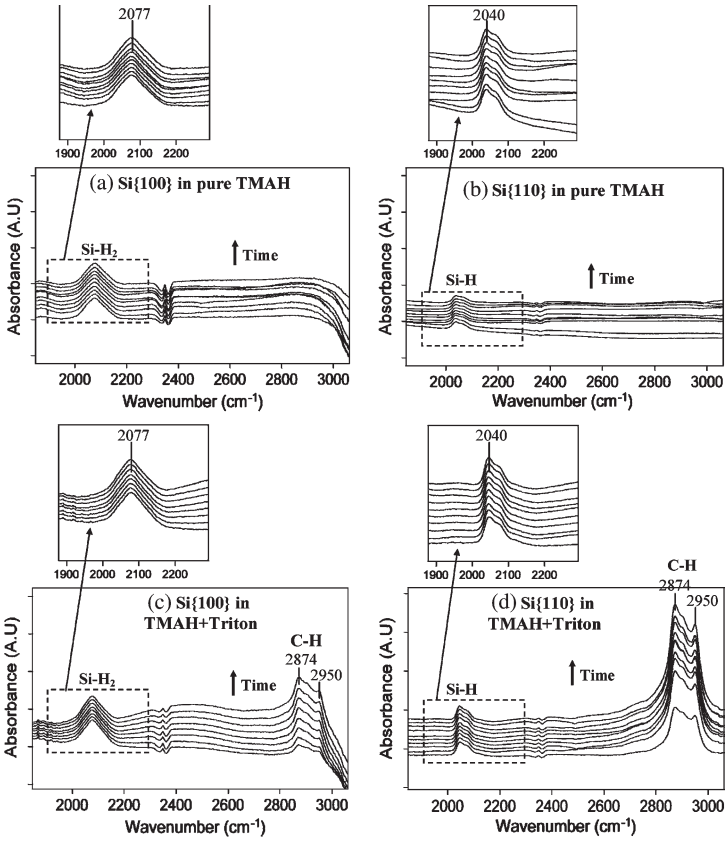

Fig. 10. IR absorption spectra in Si-H and C-H stretching vibration regions for (a) Si{100} and (b) Si{110} exposed to pure TMAH and (c) Si{100} and (d) Si{110} exposed to Triton-added TMAH. Each spectrum was collected after every 2 min during etching. Stronger adsorption of Triton molecules on {110} is observed in comparison to {100}.

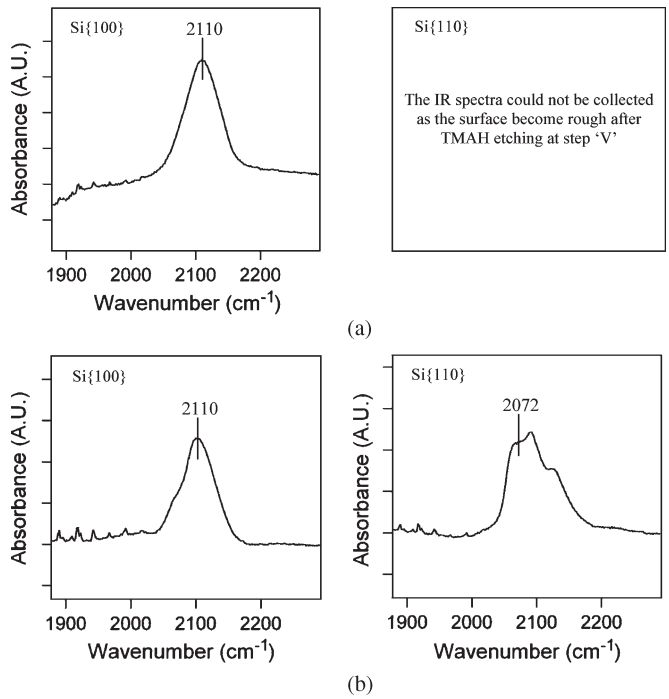

Fig. 11. IR absorption spectra in Si-H and $Si-H_2$ vibration regions for Si{100} and Si{110} exposed to DI water after etching followed by washing (performed by flowing 5% HF followed by DI water). This shows the state of surfaces after etching. (a) After etching in pure TMAH. (b) After etching in TMAH+Triton.

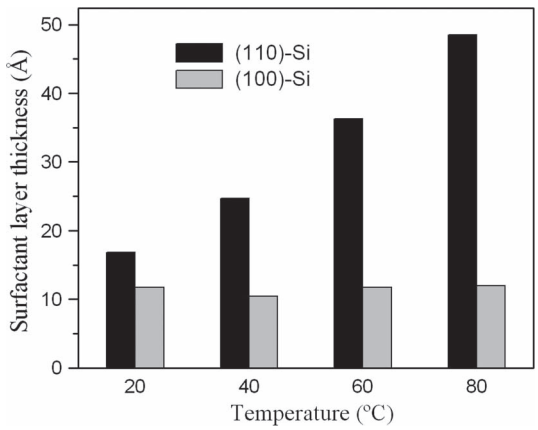

Fig. 12. Comparison of surfactant layer thicknesses on Si{110} and Si{100} adsorbed after dipping in surfactant-added DI water for 15 min followed by dipping several times in pure DI water.

water will find the H-terminated sites more comfortable while the hydrophobic ends of the surfactant molecules will find the areas between H-terminations more suitable. This argument explains that the adsorption of nonionic surfactants is larger on Si{110} than on Si{100}.

The difference in the adsorption behavior of the surfactant on the two surface orientations can be used to explain the effects on the etch rate and surface morphology. The structure of the surfactant layer is shown in Fig. 14, where the head

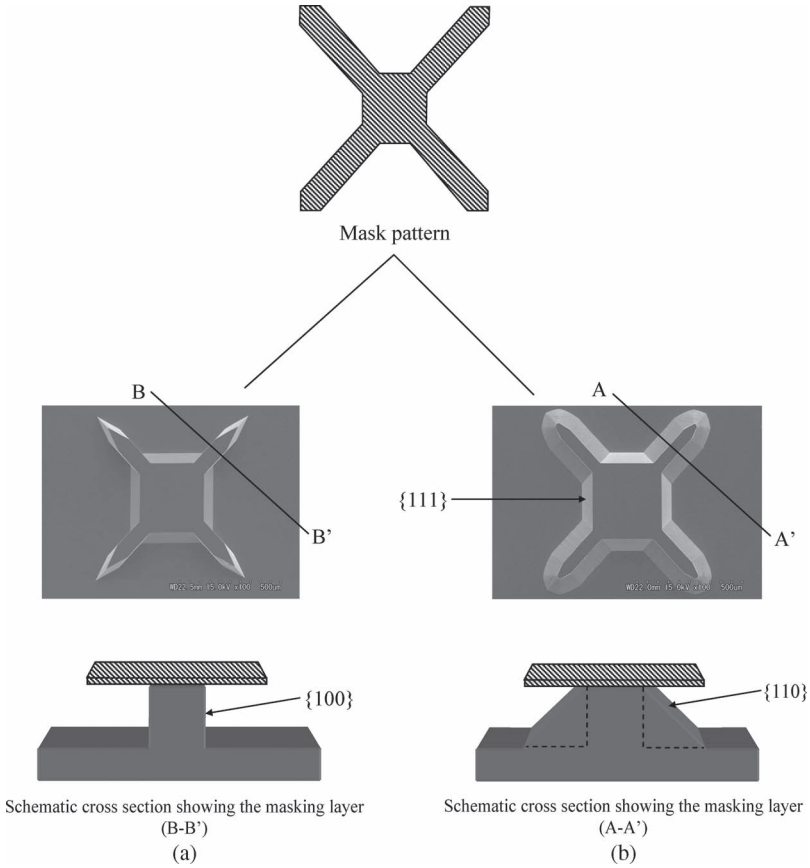

Fig. 13. Etched profile of $\langle 100 \rangle$ beams in pure and surfactant-added TMAH. (a) Pure TMAH. (b) TMAH+Triton.

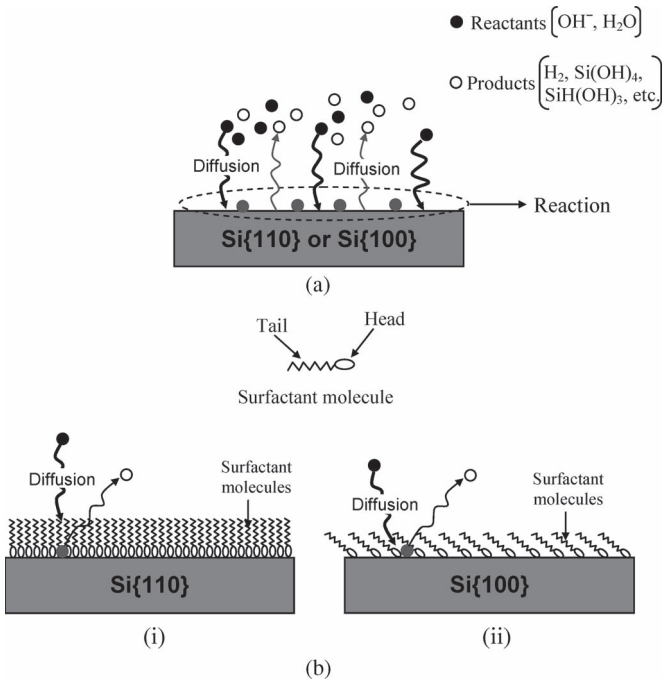

Fig. 14. Simple model representing the wet etching mechanism on silicon surface in an etchant (a) without surfactant and (b) with surfactant, for (i) Si{110} and (ii) Si{100} surfaces. The surfactant molecules adsorb more densely on Si{110} than on Si{100}, affecting the diffusion of the reactants and products significantly and resulting in a drastic reduction in the etch rate of Si{110}.

is sketched as an ellipse and the tail is sketched as a zigzag chain. The density of adsorbed molecules in the layer increases with the hydrophobic character of the surface. Likewise, the layer thickness increases with the adsorption density. As a result, more adsorption leads to a thicker layer, as schematically shown in Fig. 14. As mentioned previously, Si{110} is more hydrophobic than Si{100}, resulting in the formation of a more densely packed surfactant layer. This influences more strongly the diffusion of the reactants (i.e., OH^- and H_2O) and products (essentially H_2, $Si(OH)_4$, $SiH(OH)^3$, etc.) into and out from the etched interface, as shown in Fig. 14(b)(i). As a result, less reactants reach the surface in the presence of a thick adsorption layer, and the etch rate is correspondingly reduced. Hence, the reduction in the etch rate of Si{110} and its vicinal surfaces can be explained by considering the larger packing density of surfactant molecules on these surfaces, as compared to that of exact and vicinal Si{100}. The intense reduction of the undercutting at sharp convex [Fig. 4(a)] and rounded concave [Fig. 4(b)] corners in Triton-added TMAH can now be explained confidently as due to the higher packing density of the adsorbed layer of Triton on the $\{h\ h\ 1\}$ and $\{h+2\ \ h+2\ \ h\}$ high index planes, hindering them from the action of the etchant [see Fig. 14(b)(i)].

The strong decrease in the etch rate of exact and vicinal Si{110} reduces in turn the production of hydrogen gas (H_2). On the other hand, the presence of the surfactant layer physically covering the surface prevents the formation of large H_2

bubbles, filtering them away before they can grow too large. As a result, the surface morphology is smoothened, and the surface roughness is reduced. Similarly, the decrease in the etch rate and the physical presence of the surfactant layer result in a reduction of the amount and size of inhomogeneous regions (or inhomogeneities) in the etchant concentration and/or temperature in the close vicinity of the active regions of the surface, such as the morphological steps appearing along the zigzag morphology of {110}. These etchant inhomogeneities are the result of a time delay between the faster reaction rates at the active surface sites and the slow diffusion transport of the reactants and products in the etchant [29], [31]. The reduction in the number and size of inhomogeneities also contributes to smoothening the surface roughness. The zigzag structures typically observed on {110} due to limited diffusion transport become much shallower after the addition of the surfactants, as shown in Fig. 5(c) and (d). This is in agreement with the effect of other surfactants and alcohols on the morphology of {110} [29].

The adsorption of surfactant layers on H-terminated silicon surfaces has been studied in detail by Jeon *et al.* [16], [17], Workman *et al.* [25], and Imanishi *et al.* [26]. Jeon *et al.* focus on the study of the adsorption density of several surfactants (including Triton) as a function of surfactant concentration in solution and temperature, focusing on H-terminated Si{100} surfaces. While they characterize the adsorption and desorption characteristics of the different surfactants on this surface, the relevance for wet etching is not considered in terms of bulk micromachining applications. The work by Workman *et al.* and Imanishi *et al.* focuses on the adsorption of surfactant molecules on H-terminated Si{111} surfaces in aqueous solution, with a distant relation to silicon wet etching. Although many studies have characterized the effects of the addition of surfactants and alcohols on the etch rate and surface morphology in alkaline etchants [7]–[13], [29], according to our best knowledge, no studies have been performed to address the adsorption selectivity of these agents on different H-terminated surfaces (i.e., different orientations). In this paper, we have determined the differences in adsorption characteristics for Si{110} and Si{100} using FT-IR and ES measurements for the first time, focusing both on the mechanism and on the technological/engineering applications in MEMS.

In conclusion, all the three studies (i.e., etching characteristics for MEMS applications, *in situ* FT-IR investigation, and ellipsometry measurements) confirm the existence of surfactant adsorption selectivity on different crystallographic planes, favoring the exact and vicinal {110} surfaces. This paper sheds new light onto the mystery behind the change in the etching characteristics of pure TMAH when a very small amount of surfactant is added.

V. Conclusion

The macroscopic and microscopic aspects of pure and surfactant-added TMAH as anisotropic etchants of crystalline silicon have been presented. The macroscopic study focuses on the etching characteristics, such as the etch rates, undercutting, and surface morphologies in both etchants. This is followed by the fabrication of different shapes of MEMS structures, such as 45° mirrors, microfluidic channels, and structures with rounded concave and sharp convex corners in order to demonstrate the technological/engineering applications. The microscopic study is aimed at providing new insights on the mystery of the dramatic change in the etching characteristics of TMAH when a very small amount of surfactant is added, i.e., 0.1%-v/v Triton in this paper. The ellipsometric study of surfactant-treated surfaces and *in situ* FT-IR observation of silicon etching in pure and surfactant-added 25-wt% TMAH confirm the orientation-dependent adsorption of the surfactant. We conclude that the surfactant molecules are more densely adsorbed on exact and vicinal Si{110} than on exact and vicinal Si{100}, explaining why the etch rates of $\{110\}$, $\{h\ h\ 1\}$ and $\{h+2\ \ h+2\ \ h\}$ surfaces are considerably reduced. This reduction in the etch rates of vicinal Si{110} results in a strong suppression of the undercutting at sharp convex and rounded concave corners and at curved and non-$\langle 110\rangle$ edges.

Acknowledgment

The authors would like to thank R. Yamaguchi, N. Shimakura, and T. Muto for their technical assistance during the FT-IR measurements.

References

[1] H. Seidel, L. Csepregi, A. Heuberger, and H. Baumgartel, "Anisotropic etching of crystalline silicon in alkaline solutions I: Orientation dependence and behavior of passivation layers," *J. Electrochem. Soc.*, vol. 137, no. 11, pp. 3612–3626, Nov. 1990.

[2] A. Reisman, M. Berkenblit, S. A. Chan, F. B. Kaufmann, and D. C. Green, "The controlled etching of silicon in catalyzed ethylene–diamine–pyrochatechol–water solutions," *J. Electrochem. Soc.: Solid-State Sci. Technol.*, vol. 126, no. 8, pp. 1406–1415, Aug. 1979.

[3] M. J. Declercq, L. Gerzberg, and J. D. Meindl, "Optimization of the hydrazine–water solution for anisotropic etching of silicon in integrated circuit technology," *J. Electrochem. Soc.: Solid State Sci.*, vol. 122, no. 4, pp. 545–552, Apr. 1975.

[4] U. Schnakenberg, W. Benecke, and B. Lochel, "NH_4OH-based etchant for silicon micromachining," *Sens. Actuators A, Phys.*, vol. 23, no. 1–3, pp. 1031–1035, Apr. 1990.

[5] L. D. Clarck, J. L. Lund, and D. J. Edell, "Cesium hydroxide (CsOH): A useful etchant for micromachining silicon," in *Proc. IEEE Solid State Sensor Actuator Workshop*, Hilton Head Island, SC, Jun. 1988, pp. 5–8.

[6] O. Tabata, R. Asahi, H. Funabashi, K. Shimaoka, and S. Sugiyama, "Anisotropic etching of silicon in TMAH solutions," *Sens. Actuators A, Phys.*, vol. 34, no. 1, pp. 51–57, Jul. 1992.

[7] P. Pal, K. Sato, M. A. Gosalvez, and M. Shikida, "Study of corner compensating structures and fabrication of various shapes of MEMS structures in pure and surfactant added TMAH," *Sens. Actuators A, Phys.*, vol. 154, no. 2, pp. 192–203, Sep. 2009.

[8] C. R. Yang, C. H. Yang, and P. Y. Chen, "Study on anisotropic silicon etching characteristics in various surfactant-added tetramethyl ammonium hydroxide water solutions," *J. Micromech. Microeng.*, vol. 15, no. 11, pp. 2028–2037, Nov. 2005.

[9] P. M. Sarro, D. Brida, W. van der Vlist, and S. Brida, "Effect of surfactant on surface quality of silicon microstructures etched in saturated TMAHW solutions," *Sens. Actuators A, Phys.*, vol. 85, no. 1–3, pp. 340–345, Aug. 2000.

[10] P. Pal, K. Sato, M. A. Gosalvez, and M. Shikida, "Study of rounded concave and sharp edge convex corners undercutting in CMOS compatible anisotropic etchants," *J. Micromech. Microeng.*, vol. 17, no. 11, pp. 2299–2307, Nov. 2007.

[11] D. Resnik, D. Vrtacnik, U. Aljancic, M. Mozek, and S. Amon, "The role of Triton surfactant in anisotropic etching of {110} reflective planes on (100) silicon," *J. Micromech. Microeng.*, vol. 15, no. 6, pp. 1174–1183, Jun. 2005.

[12] E. M. Conway and V. J. Cunnane, "Electrochemical characterization of Si in tetra-methyl ammonium hydroxide (TMAH) and TMAH:Triton-X-100 solutions under white light effects," *J. Micromech. Microeng.*, vol. 12, no. 2, pp. 136–148, Mar. 2002.
[13] I. Zubel, I. Barycka, K. Kotowska, and M. Kramkowska, "Silicon anisotropic etching in alkaline solutions IV the effect of organic and inorganic agents on silicon anisotropic etching process," *Sens. Actuators A, Phys.*, vol. 87, no. 3, pp. 163–171, Jan. 2001.
[14] P. Pal and K. Sato, "Suspended Si microstructures over controlled depth micromachined cavities for MEMS based sensing devices," *Sensor Lett.*, vol. 7, no. 1, pp. 11–16, Feb. 2009.
[15] P. Pal and K. Sato, "Various shapes of silicon freestanding microfluidic channels and microstructures in one step lithography," *J. Micromech. Microeng.*, vol. 19, no. 5, pp. 055 003-1–055 003-11, May 2009.
[16] J. S. Jeon, S. Raghavan, and J. P. Carrejo, "Effect of temperature on the interaction of silicon with nonionic surfactants in alkaline solutions," *J. Electrochem. Soc.*, vol. 143, no. 1, pp. 277–283, Jan. 1996.
[17] J. S. Jeon, S. Raghavan, and R. P. Sperline, "Behavior of polyethylene oxide based nonionic surfactants in silicon processing using alkaline solutions," *J. Electrochem. Soc.*, vol. 142, no. 2, pp. 621–627, Feb. 1995.
[18] W. Haiss, P. Raisch, L. Bitsch, R. J. Nichols, X. Xia, J. J. Kelly, and D. J. Schiffrin, "Surface termination and hydrogen bubble adhesion on Si(100) surfaces during anisotropic dissolution in aqueous KOH," *J. Electroanal. Chem.*, vol. 597, no. 1, pp. 1–12, Nov. 2006.
[19] W. Haiss, P. Raisch, D. J. Schiffrin, L. Bitsch, and R. J. Nichols, "An FTIR study of the surface chemistry of the dynamic Si(100) surface during etching in alkaline solution," *Faraday Discuss.*, vol. 121, pp. 167–180, 2002.
[20] M. Niwano, M. Terashi, and J. Kuge, "Hydrogen adsorption and desorption on Si(100) and Si(111) surfaces investigated by in situ surface infrared spectroscopy," *Surface Science*, vol. 420, no. 1, pp. 6–16, 1999.
[21] M. Shinoharaa, T. Katagiri, K. Iwatsuji, Y. Matsuda, H. Fujiyama, Y. Kimura, and M. Niwano, "Oxidation of the hydrogen terminated silicon surfaces by oxygen plasma investigated by in-situ infrared spectroscopy," *Thin Solid Films*, vol. 475, no. 1/2, pp. 128–132, Mar. 2005.
[22] E. P. Boonekamp, J. J. Kelly, J. van de Ven, and A. H. M. Sondag, "The chemical oxidation of hydrogen-terminated silicon (111) surfaces in water studied in situ with Fourier transform infrared spectroscopy," *J. Appl. Phys.*, vol. 75, no. 12, pp. 8121–8127, Jun. 1994.
[23] G. J. Pietsch, Y. J. Chabal, and G. S. Higashi, "The atomic-scale removal mechanism during chemo-mechanical polishing of Si(100) and Si(111)," *Surf. Sci.*, vol. 331–333, pp. 395–401, 1995.
[24] G. J. Pietsch, Y. J. Chabal, and G. S. Higashi, "Infrared-absorption spectroscopy of Si(100) and Si(111) surfaces after chemomechanical polishing," *J. Appl. Phys.*, vol. 78, no. 3, pp. 1650–1658, 1995.
[25] A. M. A. Workman, S. Raghavan, and R. P. Sperline, "In situ ATR-FTIR analysis of surfactant adsorption onto silicon from buffered hydrofluoric acid solutions," *Langmuir*, vol. 16, no. 8, pp. 3636–3640, 2000.
[26] A. Imanishi, R. Omoda, and Y. Nakato, "In-situ FTIR studies on self-assembled monolayers of surfactant molecules adsorbed on H-terminated Si(111) surfaces in aqueous solutions," *Langmuir*, vol. 22, no. 4, pp. 1706–1710, 2006.
[27] F. Ozanam, A. Djebri, and J. N. Chazalviel, "The hydrogenated silicon surface in organic electrolytes probed through in-situ IR spectroscopy in the ATR geometry," *Electrochim. Acta*, vol. 41, no. 5, pp. 687–692, Apr. 1996.
[28] R. Atkin, V. S. J. Craig, E. J. Wanless, and S. Biggs, "Mechanism of cationic surfactant adsorption at the solid-aqueous interface," *Adv. Colloid Interface Sci.*, vol. 103, no. 3, pp. 219–304, May 2003.
[29] M. A. Gosálvez, I. Zubel, and E. Viinikka, *Wet Etching of Silicon*, V. K. Lindroos, M. Tilli, A. Lehto, and T. Motooka, Eds. Norwich, NY: William Andrew Publishing, pt. Part IV of Handbook of Silicon Based MEMS Materials and Technologies, ch. 24.
[30] M. A. Gosálvez, Y. Xing, and K. Sato, "Analytical solution of the continuous cellular automaton for anisotropic etching," *J. Microelectromech. Syst.*, vol. 17, no. 2, pp. 410–431, Apr. 2008.
[31] M. A. Gosálvez, K. Sato, A. S. Foster, R. M. Nieminen, and H. Tanaka, "An atomistic introduction to anisotropic etching," *J. Micromech. Microeng.*, vol. 17, no. 4, pp. S1–S26, Apr. 2007.
[32] V. Gutmann, *The Donor–Acceptor Approach to Molecular Interactions*. New York: Plenum, 1978.
[33] P. Jakob and Y. J. Chabal, "Chemical etching of vicinal Si(111): Dependence of the surface structure and the hydrogen termination on the pH of the etching solutions," *J. Chem. Phys.*, vol. 95, no. 4, pp. 2897–2909, 1991.
[34] B. C. Smith, *Infrared Spectral Interpretation: A Systematic Approach*. Boca Raton, FL: CRC Press, 1998.
[35] P. Allongue, V. Costa-Kieling, and H. Gerischer, "Etching of silicon in NaOH solutions II. Electrochemical studies of n-Si(111) and (100) and mechanism of the dissolution," *J. Electrochem. Soc.*, vol. 140, no. 4, pp. 1018–1026, Apr. 1993.
[36] R. A. Wind and M. A. Hines, "Macroscopic etch anisotropies and microscopic reaction mechanisms: A micromachined structure for the rapid assay of etchant anisotropy," *Surf. Sci.*, vol. 460, no. 1–3, pp. 21–38, Jul. 2000.
[37] S. Paria and K. C. Khilar, "A review on experimental studies of surfactant adsorption at the hydrophilic solid-water interface," *Adv. Colloid Interface Sci.*, vol. 110, no. 3, pp. 75–95, Aug. 2004.

Prem Pal received the B.Sc. degree in physics, chemistry, and mathematics and the M.Sc. degree in physics from Agra University, Agra, India, in 1993 and 1995, respectively, and M.Tech. degree in solid-state material and the Ph.D. degree in the area of MEMS/microelectronics technology from the Indian Institute of Technology Delhi, New Delhi, India, in 1999 and 2004, respectively.

From July 2005 to June 2006, he was a Postdoctoral Researcher with the Yonsei Microsystems Laboratory, School of Mechanical Engineering, Yonsei University, Seoul, South Korea. Since July 2006, he has been with the Sato Laboratory, Department of Micro/Nano Systems Engineering, Nagoya University, Nagoya, Japan, as a Scientist. His research interests include MEMS/microelectronics technology, MEMS-based mechanical and bio/chemical sensors, and thin films for MEMS.

Kazuo Sato (M'05) received B.S. degree from Yokohama National University, Yokohama, Japan, in 1970, and the Ph.D. degree from The University of Tokyo, Tokyo, Japan, in 1982.

He was with Hitachi Ltd. during 1970-1994. Since 1994, he has been a Professor of Micromachining and with the MEMS Laboratory, Nagoya University, Nagoya, Japan. He started MEMS research in 1983 and published more than 110 journal papers, 30 review articles, and 11 book chapters on MEMS. He is the Editor in Asia of the *Journal of Micromechanics and Microengineering* (IOP). His research areas are micro/nanophysics in anisotropic etching and mechanical properties of single-crystal silicon, as well as applied microsystems such as sensors and actuators.

Prof. Sato is a Fellow of the Japan Society of Mechanical Engineers and the Japan Society for Precision Engineering and a Senior Member of the Institute of Electrical Engineers of Japan. He cochaired the IEEE International Workshop on Micro Electro Mechanical Systems (MEMS) 1997.

Miguel A. Gosalvez received the M.S. degree (licentiate) in materials physics from the Universidad Complutense de Madrid, Madrid, Spain, in 1996 and the Ph.D. degree in computational physics from Helsinki University of Technology (HUT), Finland, in 2003.

He was a Center of Excellence (COE) Research Scientist and an Assistant Professor with the Department of Micro/Nano Systems Engineering (DMNSE), Nagoya University, Nagoya, Japan in 2004–2007 and a Postdoctoral Researcher with the Laboratory of Physics, HUT, in 2007–2008. He is currently a Global COE Research Scientist with DMNSE, Nagoya University. He is one of the two authors of VisualTAPAS (http://tfy.tkk.fi/~mag/VisualTAPAS/Home.html). His research focuses on the simulation of surface processes such as anisotropic etching, reactive ion etching, and heterogeneous catalysis using kinetic Monte Carlo and Cellular Automata methods with an aim at the fundamental understanding and the practical simulation of the processes for engineering applications.

Yasuo Kimura was born on February 8, 1972. He received the Ph.D. degree from The University of Tokyo, Tokyo, Japan, in 1999.

He is currently an Assistant Professor with the Research Institute of Electrical Communication, Tohoku University, Sendai, Japan. His research interests include fabrication of nanostructures and their applications to room-temperature operation quantum devices and solar cells.

Ken-Ichi Ishibashi was born on May 24, 1979. He received the Ph.D. degree from Tohoku University, Sendai, Japan, in 2008.

He is currently with Hang-ichi Co. Ltd, Yokohama, Japan. His research interests include fabrication of nanostructures and their applications to solar cells.

Michio Niwano was born on October 22, 1951. He received the Ph.D. degree from Tohoku University, Sendai, Japan, in 1980.

He is currently a Professor with the Research Institute of Electrical Communication, Tohoku University. His research interests include fabrication of organic devices, biosensing devices, and nanoelectronic devices.

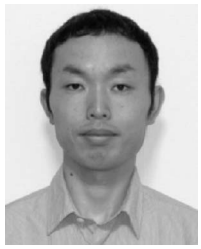

Hirotaka Hida was born in Gifu, Japan. He received the B.S., M.S., and Ph.D. degrees in mechanical engineering from Nagoya University, Nagoya, Japan, in 2003, 2005, and 2009, respectively.

He is currently an Assistant Professor with the Department of Micro/Nano Systems Engineering, Nagoya University. His research interests include scanning probe microscopies and microsensors/actuators.

Bin Tang was born in Sichuan, China, in 1982. He received the B.S. degree (optoelectronic engineering) and the M.S. degree (precision engineering) from Chongqing University, Chongqing, China, in 2005 and 2008, respectively. He is currently working toward the Ph.D. degree in the Department of Micro/Nano Systems Engineering, Nagoya University, Nagoya, Japan.

His research interests include microfabrication and microsensors and actuators.

Shintaro Itoh received the B.S. and Ph.D. degrees from Nagoya University, Nagoya, Japan, in 2001 and 2006, respectively.

He is currently an Associate Professor with the Department of Micro/Nano Systems Engineering, Nagoya University. His research areas are nanometrology and nanotribology. His research interests particularly include various kinds of solid–liquid interfacial phenomena, ranging from confined liquid between solid surfaces to molecularly thin liquid films on solid surfaces.